Preparation and photocatalytic activity of novel visible-light-driven photocatalyst Nd_2InNbO_7

KAI HAN, HONG-QI YE *, XIN-DE TANG, ZHI ZHAO, HUI LIU, YOU-FENG LI
College of Chemistry and Chemical Engineering, Central South University, Changsha, 410083, People's Republic of China

A novel visible-light-driven photocatalyst Nd_2InNbO_7 was prepared by solid-state reaction. The optical band gap of Nd_2InNbO_7 was determined to be 2.68 eV. Under visible-light irradiation, the photocatalytic activity for water splitting H_2 evolution over Nd_2InNbO_7 was higher than that over $Nd_2Zr_2O_7$. The higher photocatalytic activity of Nd_2InNbO_7 was ascribed to its conduction band nature, and the higher level of lattice distortion.

(Received April 19, 2011; accepted June 9, 2011)

Keywords: Pyrochlores, Semiconductors, Photocatalysts, Visible light, Water splitting

1. Introduction

Photocatalytic water splitting has attracted much attention since Honda and Fujishima found that clean energy carrier, H_2, can be obtained from renewable water by solar irradiation [1]. Reasonable activities for splitting water into H_2 and O_2 stoichiometrically under UV-irradiation has been achieved during the past thirty years [2-6]. However, photocatalysts responsive to visible-irradiation remain limited. It is, consequentially, desirable to develop new photocatalytic materials with high activity under visible irradiation. Some metal sulphides and (oxy)nitrides, such as RuS_2 [7], $(AgIn)_xZn_{2(1-x)}S_2$ [8], TaON [9], Ta_3N_5 [10] and $Y_2Ta_2O_5N_2$ [11], have been developed as visible light sensitive photocatalysts. Whereas, there is a deadly shortcoming of these compounds, they are unstable under light irradiation caused by the photocorrosion.Recently, a new series of visible-irradiation driven photocatalysts $Ln_2Zr_2O_7$ (Ln=Nd and Sm) have been reported [12]. These compounds possess a complex $A_2B_2O_7$-type pyrochlore structure. Pyrochlores are often written as $A_2B_2O(1)_6O(2)$ to highlight the two types of O anions present. The structure can be described as consisting of a rigid three-dimensional network of corner sharing BO_6 octahedra with the $A_2O(2)$ atoms occupying interstitial sites to form a Cu_2O-type linear network. The $B_2O(1)_6$ and $A_2O(2)$ networks weakly interact through the A–O(1) interaction and vacancies in the $A_2O(2)$ network are common place.

Herein, we report a novel oxide photocatalyst Nd_2InNbO_7 with pyrochlore structure. We consider that the B sites in the $A_2^{3+}B_2^{4+}O_7$ compound are randomly occupied by In^{3+} and Nb^{5+} ions in a charge-balanced manner, which might lead to a slight modification of the band structure and crystal structure, and resulting in a change in electrical transmission and photophysical properties. A comparison of the photocatalytic property of Nd_2InNbO_7 to that of $Nd_2Zr_2O_7$ is made under visible light. Differences are discussed from the view of relationship between structure and property.

2. Experiments

The well-crystallized Nd_2InNbO_7 powders were synthesized by the conventional solid-state method using high-purity grade chemicals In_2O_3, Nd_2O_3 and Nb_2O_5. Stoichiometric amounts of the precursors were mixed and pressed into small columns. The columns first were calcined in an aluminum crucible in air for 24 hours at 1573 K. The as-obtained column samples were reground and retreated for 48 hours at 1573 K. In the present experiment, pyrochlore $Nd_2Zr_2O_7$, which were reported to be effective photocatalysts for water splitting under visible-light irradiation. Here, it was selected references to qualitatively evaluate the photocatalytic activity of Nd_2InNbO_7. The powder of $Nd_2Zr_2O_7$ was synthesized referring to the solid-state reaction method reported [13]. The crystal structure of the powders was examined via X-ray diffraction(XRD) analysis using an X-ray diffractometer(Rigaku D/MAX–γA, Japan) by CuKα radiation. UV–Vis diffuse reflectance spectrum was measured using a UV–Vis spectrometer (TU-1901, Beijing-Purkinje, China).

Reaction for photocatalytic H_2 evolution was carried out as following: the powder catalyst (1.0g) was dispersed and suspended by a magnetic stirrer in an aqueous methanol solution (70 ml CH_3OH, 570 ml H_2O) in an outer irradiation Pyrex glass cell, which was connected to the airtight gas circulation system. The suspensions containing the samples were irradiated by a 250W Xe lamp with attached cut filters to control the wavelength of the incident light, and the amount of H_2 produced was measured by gas chromatography. For the measurements, platinum co-catalyst was loaded onto the

particle surface of photocatalysts with the photodeposition method as reported [3].

3. Results and discussion

Crystal structures of Nd_2InNbO_7 and $Nd_2Zr_2O_7$ are confirmed by XRD analysis. As shown in Fig. 1, both the as-prepared Nd_2InNbO_7 and $Nd_2Zr_2O_7$ samples were single phase. Full-profile structure refinement of the collected powder diffraction data for Nd_2InNbO_7 was performed using the Rietveld program FULLPROF [14]. Both the position parameter of refined Nd_2InNbO_7 and that of $Nd_2Zr_2O_7$ were shown in Table 1, which indicated that Nd_2InNbO_7 and $Nd_2Zr_2O_7$ are crystallized in cubic system with space group Fd3m, and the lattice parameter is a=10.6027(3) and 10.648 Å, respectively. All of the reflection peaks could be successfully indexed based on the lattice parameter and the space group (see Fig. 1). The UV-Vis diffuse reflectance spectrum of Nd_2InNbO_7 is illustrated in Fig. 2. The optical band gap of Nd_2InNbO_7 is found to be 2.68 eV, the band gap energy of $Nd_2Zr_2O_7$ was evaluated [12] to be 2.53 eV by photoelectrochemical method.

Table 1. The crystal structural data of Nd_2InNbO_7 and $Nd_2Zr_2O_7$.

(a) Crystal structure					
		Crystal system	Space group	Lattice parameter (Å)	
Nd_2InNbO_7		Cubic	Fd3m	10.6027(3)	
$Nd_2Zr_2O_7$ [a]		Cubic	Fd3m	10.648	
(b)Atomic position					
	atom	x	y	z	Lattice distortion
Nd_2InNbO_7	In/Nb	0	0	0	0.0400(6)
	Nd	0.5	0.5	0.5	
	O(1)	0.3326(5)	0.125	0.125	
	O(2)	0.375	0.375	0.375	
$Nd_2Zr_2O_7$ [a]	Zr	0	0	0	0.0423(5)
	Nd	0.5	0.5	0.5	
	O(1)	0.3349(4)	0.125	0.125	
	O(2)	0.375	0.375	0.375	

[a]Ref [12]

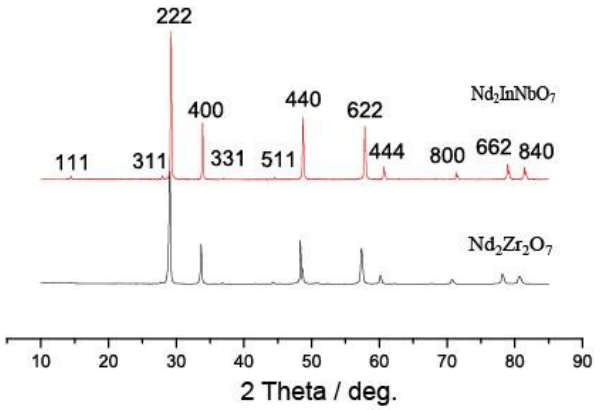

Fig. 1. X-Ray diffraction patterns of Nd_2InNbO_7 and $Nd_2Zr_2O_7$.

The H_2 evolution as a function of visible-light irradiation time is shown in Fig. 3. After 10 h of light illuminating, the total amount of evolved H_2 over Nd_2InNbO_7 is 4.1 μmol, which is higher than 2.6 μmol over $Nd_2Zr_2O_7$. Further more, for the Pt-loaded Nd_2InNbO_7 (0.1 wt %), the generated amount of H_2 reaches 45.5 μmol. Fig. 4 presents the H_2 evolution over Nd_2InNbO_7 and Pt-loaded Nd_2InNbO_7 under visible-light irradiation. Within 10h of visible light irradiation, the average rate of H_2 evolution over Nd_2InNbO_7 is 0.41 μmol/h. The respective average rate of H_2 evolution over 0.05 wt% and 0.2 wt% Pt-loaded Nd_2InNbO_7 increases to be 1.8 and 2.4 μmol/h, and the 0.1 wt% Pt-loaded sample possesses a highest average rate of H_2 evolution, 4.5 μmol/h. It is well-known that the Pt/semiconductor composite leads to the formation of a Schottky barrier. Thus, the photoinduced electrons in the conduction band of the semiconductor are believed to readily transfer to Pt, which facilitates the separation of the photogenerated electron-hole pair and resulting in an improved the photocatalytic activity.

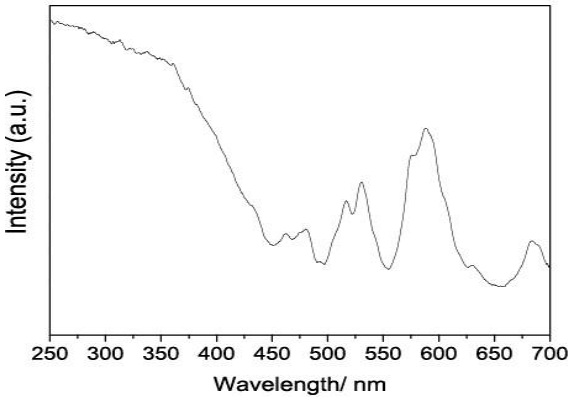

Fig. 2. UV–Vis diffuse reflectance spectra of Nd_2InNbO_7.

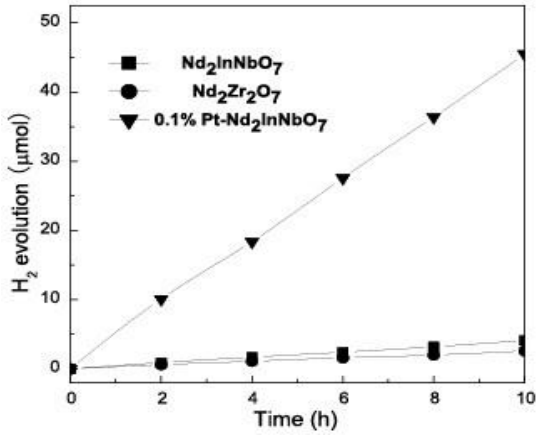

Fig. 3. Photocatalytic activities of 0.1%Pt-Nd_2InNbO_7, Nd_2InNbO_7 and $Nd_2Zr_2O_7$.

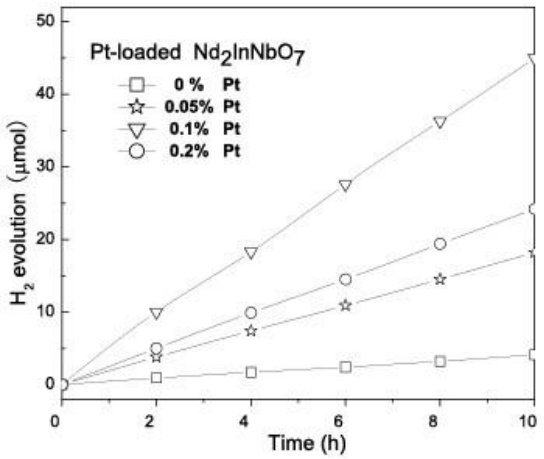

Fig. 4. Photocatalytic activities of Pt/ Nd_2InNbO_7.

Hence, 0.1 wt% Pt is loaded onto Nd_2InNbO_7 and $Nd_2Zr_2O_7$ particles, respectively. Their comparative results of H_2 evolution under visible-light are shown in Fig. 5. The reaction is repeated three times.

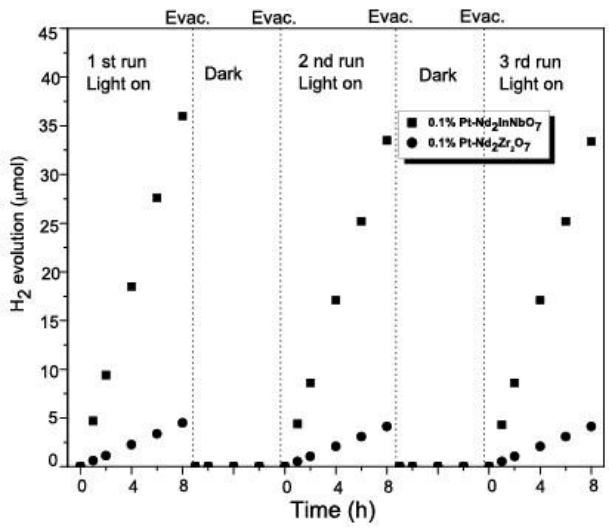

Fig. 5. Photocatalytic activities of 0.1% Pt-Nd_2InNbO_7 and 0.1% Pt-$Nd_2Zr_2O_7$.

Clearly, the amounts of evolved H_2 increase linearly with an increase of irradiation time in three runs. The photoactivities over Nd_2InNbO_7 and $Nd_2Zr_2O_7$ slightly decrease in the second run, but no further attenuation occurred in the third run. The XRD pattern of Nd_2InNbO_7 shows no difference before and after the photocatalytic H_2 evolution, indicating the Nd_2InNbO_7 compound is stable under the present working condition. The average rate of H_2 evolution in the third run is 4.2 and 0.56 μmol/h for 0.1 wt% Pt-loaded Nd_2InNbO_7 and 0.1 wt% Pt-loaded $Nd_2Zr_2O_7$, respectively. No H_2 is detected when the light was turned off ('dark test') and the reaction cell is re-evacuated. This result excludes the possibility of H_2 generation from the 'mechano-catalytic mechanism' [15].

It is generally believed that the band structures of photocatalyst play an important role in the photocatalytic activities. Prokofiev et al. [16] had studied periodicity in the optical band gap variation of rare earth sesquioxides. According to their results, the occupied 4f band in rare earth sesquioxides lay above the O2p level, and thus the 4f-d transition determined the band gaps. Consequently, the Nd4f orbital exist above the top of the O2p orbital and the valence band edge of $Nd_2Zr_2O_7$ become higher to decrease band gap energy (E_g). The same consideration may be made for the Nd_2InNbO_7 compound. Recently, the electronic structures of $InNbO_4$ photocatalysts have been reported by Oshikiri et al. based on the first principles calculations [17]. The conduction bands of the $InNbO_4$ photocatalysts consist of a small In5s orbital component and a dominant Nb4d orbital component. The band structures of the Nd_2InNbO_7 and $Nd_2Zr_2O_7$ photocatalysts are suggested according to the above reports. Their valence band should consist of Nd4f and O2p orbitals, and their conduction band should consist of Nb4d and In5s for Nd_2InNbO_7 and Zr4d orbital for $Nd_2Zr_2O_7$, respectively. Fig. 6 shows suggested band structures of the Nd_2InNbO_7 and $Nd_2Zr_2O_7$ photocatalysts. Our simple assumption is that the narrower band gap of Nd_2InNbO_7 and its conduction band nature may result in a larger amount of light absorption and lower recombination rate of charge carrier, comparing to that of $Nd_2Zr_2O_7$.

It is also believed that the crystal structures of photocatalyst with similar band structure play a crucial role in the photocatalytic activities.

The distortion of BO_6 polyhedra in $A_2B_2O_7$-type pyrochlore structures results in their lattice distortion which is one of the important parameters for charge separation and contributes to enhance the photocatalytic activity [18,19]. The correlation between photocatalytic activity and lattice distortion has been demonstrated in a series of pyrochlore-type structure metal oxide photocatalysts [20,21]. Information on the lattice distortion can be obtained from the O(1) parameter x in the pyrochlore-type $A_2B_2O_7$ structure. The lattice distortion is equal to 0.375 − the O(1) parameter x. For $Nd_2Zr_2O_7$, x=0.3349(4), the lattice distortion is evaluated to be 0.0400(6) while that for Nd_2InNbO_7 photocatalyst is evaluated to be 0.0423(5). Thus, the present results of the Pt-loaded Nd_2InNbO_7 showing high photocatalytic performance are in line with the correlation between activity and lattice distortion.

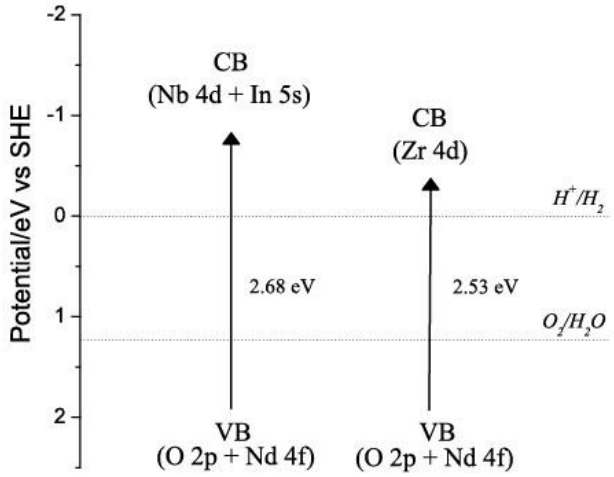

Fig. 6. Suggested band structures of Nd_2InNbO_7 and $Nd_2Zr_2O_7$.

4. Conclusions

Novel Nd_2InNbO_7 powder was synthesized via a solid-states reaction method. Photocatalytic activity for water splitting over Nd_2InNbO_7 was higher than that over $Nd_2Zr_2O_7$ under visible-light irradiation. The predominant photocatalytic activity that Nd_2InNbO_7 exhibiting was ascribed to its conduction band nature and heavier lattice distortion, generating by co-occupation of In^{3+} and Nb^{5+} in B site of pyrochlore-type $A_2B_2O_7$ compound.

This work was financially supported by the Research Fund for the Doctoral Program of Higher Education (200805330032).

References

[1] A. Fujishima, K. Honda, Nature, **238**, 37 (1972).
[2] R. Asahi, T. Morikawa, T. Ohwaki, K. Aoki, Y. Taga, Science, **293**, 269 (2001).
[3] H. Kato, K. Asakura, A. Kudo, J. Am. Chem. Soc., **125**, 3082 (2003).
[4] H. Kato, A. Kudo, Catal. Today, **78**, 561 (2003).
[5] K. Sayama, A. Tanaka, K. Domen, K. Maruya, T. Onishi, J. Phys. Chem. B, **95**, 1345 (1991).
[6] J. Sato, N. Saito, H. Nishiyama, Y. Inoue, J. Phys. Chem. B, **15**, 6051 (2001).
[7] K. Hara, K. Sayama, H. Arakawa, Applied Catalysis *A:* General, **189**, 127 (1999).
[8] I. Tsuji, H.Kato, H. Kobayashi, A. Kudo, J. Am. Chem. Soc, **126**, 13406 (2004).
[9] M. Hara, G. Hitoki, T. Takata, J. N. Kondo, H. Kobayashi, K. Domen, Catal. Today, **78**, 555 (2003).
[10] G. Hitoki, A. Ishikawa, T. Takata, J. N. Kondo, M. Hara, K. Domen. Chem. Lett., **6**, 736 (2002)
[11] M. Liu, W. You, Z. Lei, G. Zhou, J. Yang, G. Wu, G. Ma, G. Luan, T. Takata, M. Hara, K. Domen, C. Li, Chem. Commun., 2192 (2004).
[12] M. Uno, A. Kosuga, M. Okui, K. Horisaka, H. Muta, K. Kurosaki, S. Yamanaka, J. Alloys Compd., **420**, 291 (2006).
[13] H. Yamamura, H. Nishino, K. Kakinuma, J. Phys Chem Sols., **69**, 1711 (2008).
[14] J. Rodriguez-Carvajal, Fullprof 2k, Version 3.4 (Nov. 2005), Laboratoire Leon, Brillouin (CEA/CNRS), CEA-Saclay, 91191 Gifsur-Yvette Cedex, France.
[15] K. Domen, J. N. Kondo, M. Hara, T. Takata, Bull. Chem. Soc. Jpn., **73**, 1307 (2000).
[16] A. V. Prokofiev, A. L. Shelykh, A. V. Golubkov, I. A. Smirnov, J. Alloys Comp., **219**, 72 (1995).
[17] M. Oshikiri, M. Boero, J. Ye, Z. Zou, G. Kido, J. Chem. Phys., **117**, 7313 (2002).
[18] Z. Zou, J. Ye, H. Arakawa, J. Mater. Sci. Lett., **19**, 1987 (2000).
[19] Y. Inoue, M. Kohno, S. Ogura, Chem. Phys. Lett., **267**, 72 (1997).
[20] A. Kudo, H. Kato, S. Nakagawa, J. Phys. Chem. B, **104**, 571 (2000).
[21] J. Wang, Z. Zou, J. Ye, J. Phys Chem. Sols., **66**, 349 (2005).

*Correspoding author: csuhankai@gmail.com, hongqiye@gmail.com